Quantifying spatial and angular resolution of light field 3D displays

Péter Tamás Kovács, *Student member, IEEE*, Robert Bregović, *Member, IEEE*, Atanas Boev, Attila Barsi, and Atanas Gotchev, *Member, IEEE*

***Abstract*— Light field 3D displays are expected to play an important role as terminal devices, visualizing 3D objects apparently floating in the air, or letting viewers see through a window with a scene behind it. Currently, there are neither methods nor practical tools to quantify light field display's effective resolution or the perceived quality of the presented imagery. Most 3D displays are simply characterized by the total number of pixels or light rays; however this number does not properly characterize the distribution of the emitted light rays, nor the level of detail that the display can visualize properly. This paper presents methods to measure the spatial (i.e. 2D equivalent) and angular (i.e. directional) resolution of a given light-field display. The frequency domain analysis of recorded test patterns gives the spatial resolution limit of the display under test, while angular resolution is determined by the display's ability to pass through patterns of uniform, angle dependant patterns. It also presents a subjective experiment to corroborate the objectively measured spatial resolution.**

***Index Terms*—Displays, Three-dimensional television, Image resolution, Spatial resolution, Distortion, Spectral analysis**

I. Introduction

VISUAL information has always been the primary and richest kind of information perceived by humans. Consequently, displays are primary output devices of computers and other electronic devices, including handheld, desktop and large-scale surfaces for representing visual information, some of which have 3D capabilities in recent products. Examples include 3D enabled phones, TVs and computer monitors. With recent advances in display technology, users expect immersiveness and realism when perceiving and interacting with visual information. Thus, displays are aimed at reproducing an increasing subset of visual cues present in reality: vivid colors, high resolution, binocular effect (when two eyes see different images, resulting in stereopsis), and the parallax effect (when an observer can see different perspectives while moving in front of the screen) all contribute to a higher realism of the displayed information [1]. Reproducing binocular effects and motion parallax are unique to autostereoscopic (glasses-free) 3D displays, which are implemented based on various technologies, such as lenticular-lens based multiview [2] or projection-based light-field displays [3][4][5][6].

A. Motivation

Given different display technologies and models, one needs quantitative measures in order to know what to expect from a given display, what they can deliver in terms of visual realism. The characterization of the throughput of light-field 3D displays is an important yet challenging issue [7].

In case of 2D displays, spatial resolution is one of the major factors affecting visual realism, and is equally important for 3D displays. However, most 3D display manufacturers describe their products using metrics originating from 2D displays, such as the resolution of the underlying display panel, which does not quantify the distribution of these pixels in the spatial / directional domain. Light-field displays do not have a regular pixel structure, as will be described in Section II.A. Therefore measuring the number of features that can be faithfully represented by the display on the screen plane from a single viewing position (i.e. equivalent spatial resolution) is an important metric to judge the visual quality and level of detail presented by the 3D display. The effective resolution away from the screen plane (that is, for content that appears inside the display, or floating in front of the screen) can be calculated from the resolution at the surface using geometrical considerations [3].

Angular resolution is a new metric specific for 3D displays. It does not exist for 2D displays, as those do not exhibit viewing angle dependent behavior. For 3D displays, angular resolution quantifies the quality of the parallax effect. Visible discrete transitions in the motion parallax caused by insufficient angular resolution can hinder viewing experience and may hide important details of the presented information. The smoothness of motion parallax largely depends on the number of rays one can see over unit length when moving in front of the display's screen. Even more importantly, angular resolution has a direct effect on the depth range, that is, the range of depth shown with reasonable image quality. By

Manuscript received XXX; accepted XXX. Date of publication XXX.

The research leading to these results has received funding from the PROLIGHT-IAPP Marie Curie Action of the People programme of the European Union's Seventh Framework Programme, REA grant agreement 32449. Participants of the subjective experiment are gratefully acknowledged.

P. T. Kovács is with Tampere University of Technology, Tampere, Finland and Holografika, Budapest, Hungary (e-mail: peter.t.kovacs@tut.fi).

R. Bregović is with Tampere University of Technology, Tampere, Finland (e-mail: robert.bregovic@tut.fi).

A. Boev is with Tampere University of Technology, Tampere, Finland and Huawei ERC, Munich, Germany (e-mail: atanas.boev@huawei.com).

A. Barsi is with Holografika, Budapest, Hungary (e-mail: a.barsi@holografika.com).

A. Gotchev is with Tampere University of Technology, Tampere, Finland (e-mail: atanas.gotchev@tut.fi).

measuring the angular resolution, we are indirectly measuring the maximum depth that can be shown on the display [3].

Spatial and angular resolutions together imply the properties and the necessary processing [8] of the light field content the display should be supplied with.

B. Organization of this paper

In this paper we propose methodologies for objective measurements to quantify spatial and angular resolutions. Furthermore, we propose and conduct subjective tests to corroborate the results of the spatial resolution measurements. Angular resolution measurement results are validated by technology insights from the display used in the experiments.

The rest of this paper is organized as follows. Section II describes related work in display measurement and briefly introduces light field displays (the 3D display technology this paper is focused on), and the concept for estimating display passband based on the display's geometry. Section III describes the objective measurement methods and how the results are analyzed to calculate spatial and angular resolutions, while Section IV describes the subjective test aimed at corroborating the objective measurement results. Section V presents sample results for a specific light-field display and compares the measurement results with the results of subjective experiment. Section VI concludes the paper.

II. Related work

A. Light-field 3D displays

Projection-based light-field 3D displays as described by Balogh [3] aim to reproduce the light-field of a real or synthetic scene by creating a surface with direction selective light emission. This is achieved by stacking many projection modules in a regular arrangement, so that these modules project light rays onto the screen, typically from behind. All projection engines beam light rays onto the whole screen area and these light rays hit the screen surface in slightly different directions. The special holographic screen onto which the rays are projected lets these rays pass through without changing their direction or mixing the color of the different light rays, as shown in Fig. 1.

The holographic screen applies a limited amount of horizontal diffusion, effectively applying discrete-to-continuous conversion on the discretized sources of light [9].

Using such optical arrangement, it is possible to show different images of the same scene to slightly different directions, so that the two eyes of the viewer can see different perspectives, resulting in stereopsis. Also, yet other images are shown to other directions that are seen when the viewer is moving in front of the screen, resulting in motion parallax. The number of different directions emitted from a single screen position can vary and reproducing hundreds of directions is not uncommon. The color of each light ray emitted by the projection modules is determined based on the light field to be represented, and the geometry of the optical arrangement by sampling the desired light field.

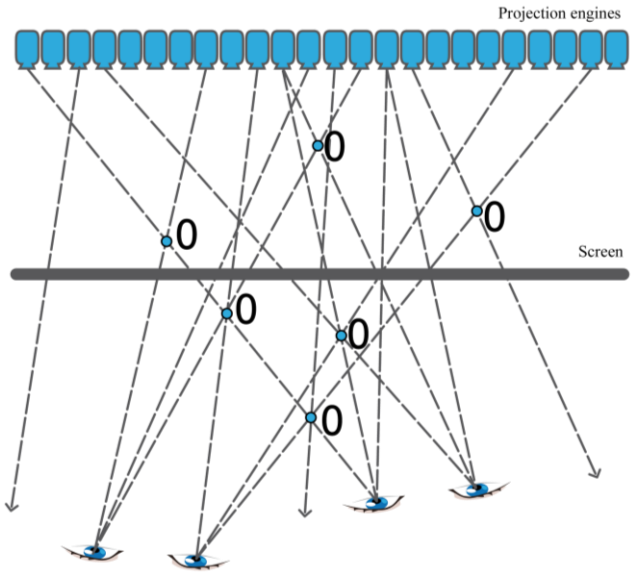

Fig. 1. Principle of operation of projection-based light-field 3D displays. Projection engines project light rays from behind, which may cross each other behind or in front of the holographic screen.

The light field is reproduced up to a certain spatial and angular resolution, upper bounded by the total number of light rays emitted by the display.

Projection engines are computer controlled, and thus generating and outputting arbitrary light-fields is possible by software means. The methods described in the next sections are supported by software for generating test light-field patterns, as well as for capturing and analyzing the displayed patterns.

B. Limiting factors of light-field displays

There are factors that impose an upper limit on the capabilities of projection-based light-field displays, as well as other factors that can affect the final perceived image quality. First, the projection engines generating the light rays, typically containing an imaging component like DLP (Digital Light Processing) or LCoS (Liquid Crystal on Silicon), have finite resolution, such as VGA, XGA, WVGA, HD, or 4k, posing an upper limit on the number of light rays emitted from a single source.

Mounting a large number of projection engines requires a mechanical system, which cannot always ensure pixel-precise matching of light ray hit points on the screen. As a result, positional and rotational misalignments may occur. Also, the optical system of projection engines might have lens distortions, resulting in a non-perfectly rectangular image with equally spaced pixels. While these distortions can be compensated by measuring and pre-distorting the light field, sub-pixel differences still occur, resulting in light rays emitted at fractional positions. Because of this, an observer cannot count pixels on a light-field display's screen in the way it is possible on a 2D display having a discrete pixel structure.

The finite number of projection engines implies that the number of different directions reproduced is finite, and thus angular resolution has a limit.

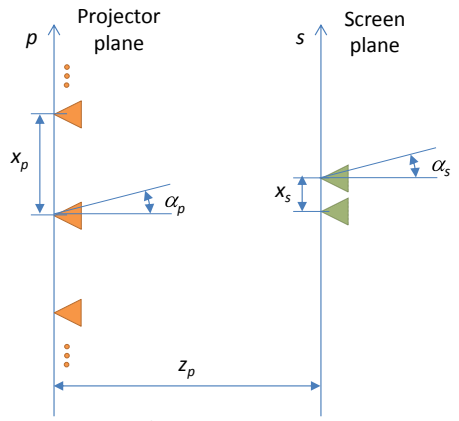

Fig. 2. Projection based light field display setup with notations.

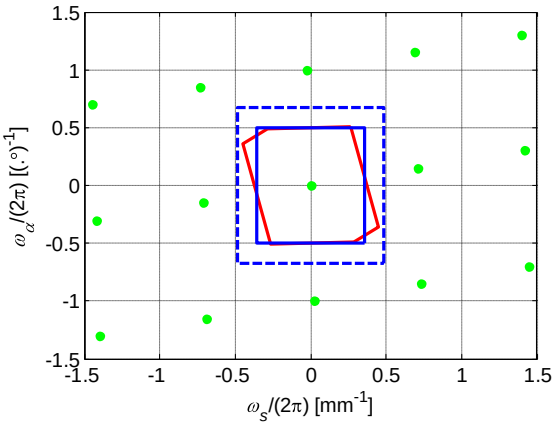

Fig. 3. Frequency domain sampling pattern (green) with estimated display passband (red) and shapes of different diffusors (blue).

While one projection engine can contribute to multiple emitted directions simultaneously using side mirrors which reflect a subset of light rays back to the screen from angles not covered by projection engines, the maximum number of directions cannot be higher than three times the number of projection engines in the system in case of a Horizontal Parallax Only (HPO) system (center, left reflection, right reflection).

C. *Display passband*

Spatial and angular resolution are parameters of a more general concept, namely the bandwidth or passband of the display [10]. The passband characterises the display as a light field generator in Fourier domain and as such contains those frequencies, both in the spatial and angular domain (or, equivalently in the ray phase-space domain), which the display is able to reproduce without excessive spatial or inter-perspective aliasing.

As demonstrated in our previous work [9], the passband of a projection-based light field display can be estimated based on the geometrical configuration of the display and applying light field formalism on the display-generated light field. In practice, this requires knowledge about the properties and position of the projection engines and the screen (diffusor). Such approach is particularly useful when designing a display. Based on the desired light field, one can determine the optimal configuration of the display optical elements (which in turn can then be followed by determining optimal camera setup and the necessary pre-filtering) for approximating that desired light field.

In either case (building a display or evaluating the properties of an existing display), the assumption is that the reconstruction support of the diffusor in Fourier domain follows the optimal passband shape. However, in practice, the diffusor cannot have arbitrary shape. It is more-or-less restricted to rectangular shape similar to the ones discussed in [9]. The geometrical analysis considers the ray (spatial-angular) positions and interpret them as sample positions in ray space. As such, it enables estimating the preferable (optimal) reconstruction filter at the diffusor plane.

For illustrative purpose we present here an example. Consider a projection-based display with 22 cpd (cycles per degree) resolution at viewing distance of 3.5 m having 70 views over a field-of-view of 70 °.[1]

Following the notations in Fig. 2, this corresponds to spatial-angular sampling at the display plane such that $(x_s, \alpha_s) = (1.40\ \text{mm}, 1\ °)$. Rewriting the relation between the plane with projection units and the screen plane (see Eq. 14 in [9]), the parameters describing the sampling grid on the projection plane are evaluated as

$$\alpha_p = \text{atan}\left(\frac{x_s}{z_p}\right) \text{ and } x_p = \frac{\alpha_s}{\alpha_p} x_s.$$

Selecting the distance between screen and projection units as $z_p = 2500\ \text{mm}$, the display parameters are estimated as $(x_p, \alpha_p) = (43.633\ \text{mm}, 0.0321\ °)$. By performing the analysis as proposed in [9] one obtains sampling pattern in the Fourier domain as shown in Fig. 3. On the same figure, the display passband is shown in red, that in turn would be the optimal shape for the reconstruction filter of the diffusor. In practice the diffusor's Fourier-domain bandwidth is more like the ones of the blue squares with the one shown with solid line being the best candidate for the given sampling pattern. It offers the best overlap with the display bandwidth as determined by the geometry of the ray generators. A diffusor with wider bandwidth would imply worsened spatial selectivity of rays and diffusor with a narrower Fourier-domain support would be unnecessarily restrictive thereby removing finer details.

In summary, there are two issues with the theoretical analysis based on the configuration of optical elements: first, the need to know the correct physical configuration and, second, to know the properties of the diffusor. From the point of view of a general display user, these are not provided by the manufacturer. Then, the practical solution is to measure the parameters of the display passband in a way that would include the real contribution of all elements building the

[1] The display has been selected such to be close to the real display that will be measured / analyzed later on and for which the real geometrical data is not available.

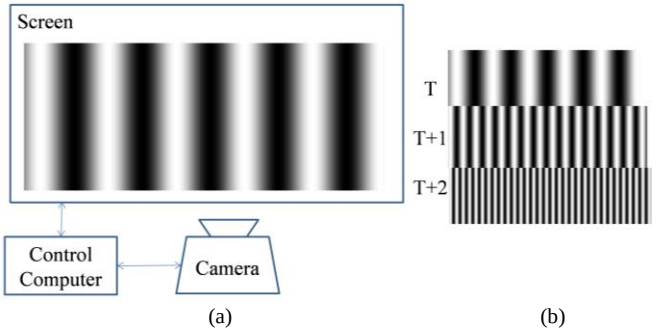

Fig. 4. Spatial resolution measurement overview. (a) A sinusoidal test pattern is rendered on the display under test, while a camera attached to the control computer takes a photo. (b) Subsequent measurement iterations show sinusoidals with increasing frequency.

display. Two measurement approaches aimed at this are introduced in this paper.

D. 3D Display measurement and quantification

Most previous work on 3D display measurement have targeted the measurement and quantification of stereoscopic and multiview displays. Boev et al. developed a method [11] for modeling multiview displays in the frequency domain and identifying their limits using test patterns of different orientation and frequency. Their work, however only applies to multiview displays and only concerns spatial resolution.

Boher et al. developed measurement equipment using Fourier optics to measure the views emitted by desktop multiview displays [12]. While this gives precise results for the targeted class of displays, its applicability for large-scale 3D displays, as well as light-field displays using front projection is rather limited due to the size of the equipment and the way it is used (it would block the light path).

The International Display Measurement Standard (IDMS) published by the Society for Information Display [13] provides guidelines for measuring spatial and angular resolution of 3D displays in general. The recommended angular resolution measurement method relies on showing two-view patterns, which is not applicable for light-field displays, as these do not have discrete views to be controlled. It is also assumed that pixel size is known, which cannot be ensured when measuring an unknown display, which limits the applicability of this method. It further implicitly assumes that the pixels are rectangular, which is not true for several projection technologies (for example diamond shaped pixels in some DLPs).

From the methods presented in the IDMS for spatial resolution measurement for 2D displays, "Resolution from contrast modulation" is probably the closest to our method. This method uses grille lines of discrete sizes and measures the contrast ratio for these patterns. The effective resolution is estimated based on where the contrast ratio is expected to fall below 50%, which is typically located between two discrete measurements. Our method is more precise, because on LF displays patterns with arbitrary size can be shown, thus interpolation is not necessary. The other advantage of our method is that it does not rely on contrast ratio only, but takes into account other sources of noise than decrease in image contrast (regardless of its source).

The authors are not aware of any comprehensive measurement method capable of quantifying spatial and angular resolution of light-field displays or any other 3D display with irregular pixel structure. Our previous work [14] presented an earlier version of spatial resolution measurement of light-field displays and an early method for angular resolution measurement, which used intensity loss for characterizing angular resolution. In this work we expand it by applying frequency analysis for characterizing angular resolution.

III. MEASUREMENT METHODOLOGY

A. Methodology for spatial resolution measurement

Our aim is to devise a methodology for measuring the equivalent spatial resolution of a light-field display using commodity camera and processing tools. The approach is inspired by the methodology presented in [11] for the case of multi-view displays. The measurement is accomplished by (1) visualizing sinusoidal test patterns with different frequency; (2) capturing the visible output by a camera; (3) analyzing the captured images in the frequency domain in order to check if the display reproduces the intended pattern without excessive distortions, and (4) converting frequencies to equivalent spatial resolution.

The test patterns are rendered with custom software that colors each light ray based on the hit point with the display's screen, regardless of its angle.

The rendered test pattern is a black-white sinusoidal that is shown over the whole screen surface (see Fig. 4. (a)), initially showing only a few periods on the screen. The attached camera takes a photo of the pattern as shown on the display, and the frequency of the sinusoidal is increased (see Fig. 4. (b)). The process is repeated until the frequency of the sinusoid well exceeds the theoretical limit of resolution of the light-field display, which is determined by the resolution of the imaging components. We use frequencies which are up to twice higher than the frequency corresponding to the maximum resolution of the imaging components. The same measurement is repeated for vertical sinusoidals.

The camera recording the test patterns as they are shown is set up on a tripod facing the display; the height of the sensor matches the center of the screen, and the use of manual shooting settings to ensure the captured intensity range matches the brightness of the display, so that the blacks and whites in the displayed patterns are visible on the photos (not saturating the dynamic range of the camera). The camera must be set to a resolution at least 2x times higher than the theoretical maximum resolution of the display (in practice, our algorithm uses four times as many samples to oversample the picture, considering any possible super-resolution effects caused by the multi-projection system). The shutter speed must be slower than the time-multiplexing frequency of the projection components (as projection engines typically employ

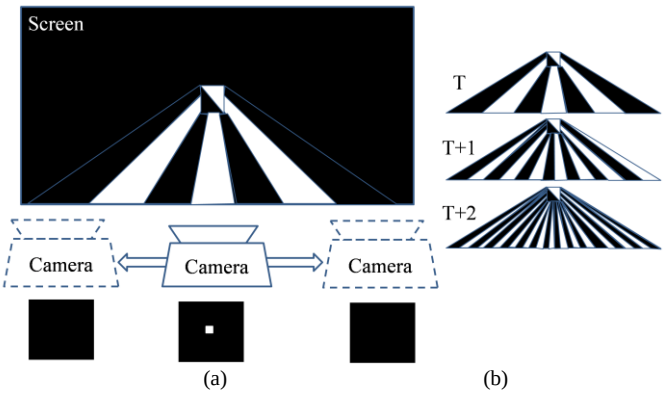

Fig. 5. Angular resolution measurement overview. (a) Test setup with moving camera. The rectangle looks black from some locations and white from other locations. (b) Test patterns of increasing angular frequency.

time multiplexing to emit R, G and B color components using a single imaging component; this frequency is available in the projection engine's data sheet), and the camera focus is set on the screen plane.

B. Analysis of spatial resolution

The analysis of the photos of spatial resolution measurement is based on the observation that the frequency spectrum of the cropped photos, showing only the sinusoidal patterns and the distortions introduced by the display, clearly indicates the limit where the display is incapable of reproducing the test pattern. The test pattern is displayed on the whole screen, photographed, and 1D frequency analysis is performed on a single line of samples in the center of the screen. By increasing the frequency, the amplitude of the dominant frequency decreases, while at the same time distortion and after a certain frequency aliasing are introduced.

The algorithm determines the limit of resolution where the amplitude of distortion exceeds 20% of the amplitude of the dominant frequency. The horizontal spatial resolution then matches with the number of transitions of the test pattern that has been shown before the threshold was exceeded. The 20% threshold is associated with the level of disruptive distortion - this is the level of distortion (originating from aliasing or other nonlinear effects) which makes it impossible for the viewer to precisely identify all features of the presented visual data. The arguments for selecting 20% threshold came from [15], which in turn took insights from previous works, that had reported 10% [16], 15% [17], and 25% [18], respectively.

The same analysis is repeated for the orthogonal direction.

C. Methodology for angular resolution measurement

For performing the desired measurements, one needs to emit different colors or intensities to different directions, and measure the screen from various angles. For a relatively small field of view produced by multiview displays, this may be accomplished by placing a relatively large sensor close to the screen as done in [12], but for the wider field of view typically produced by light-field displays, a moving camera is necessary.

On the display side, one needs to present a light field that has a well recognizable part that looks differently when observed from different angles (see Fig. 5. (a)).

In practice, the renderer driving the display uses a GPU shader that receives the parameters of the ray to be colored as input, based on which it calculates the position of the hit point on the screen and forms a rectangle-shaped measured spot. It also calculates the emitted direction, according to which rays are colored either black or white. The screen area that is colored in this way appears black from some viewing angles, and appears white from others, alternating as the observer or camera moves sideways. A camera moving in parallel with the screen plane records the transitions on video, the frames of which are subsequently analyzed. The setup of the camera is similar to that of the spatial resolution test, but the camera is mounted on a motorized rig that allows precise positioning of the camera.

In subsequent measurement iterations the angle of black / white features is decreased, thus more transitions are emitted per unit angle, and a new sliding video is recorded (see Fig. 6. (b)).

There is a possibility to check the angular resolution relying on information about the engine's order and topology in case of projection-based light-field displays, determining the maximum number of distinct light ray directions that can be emitted. Knowing the order of optical engines, one can force every even projection unit to project white, and odd ones to project black. This presents an intensity profile, while reversing the pattern presents the complement of this profile. Overlaying the two profiles shows peaks at every distinct direction that can be reproduced, and these peaks can be counted (see Fig. 10. (b) for an example, where one profile is shown for clarity). As no light can originate from between two discrete light sources inside the display, this limit cannot be exceeded by any test pattern. As our aim is to devise a general methodology for measuring the angular resolution, we use this alternative only to validate the first approach, which in turn requires no direct control of individual projection engines.

D. Analysis of angular resolution

The display is considered to be capable of showing the pattern with the given angular resolution if the black / white transitions can be still recognized. In our analysis this is formulated by maximum achievable frequency in the directional domain. As we increase the angular frequency of the test pattern, we can observe that the transitions are still present; however, after a given frequency, the analysis shows that the dominant frequency is disappearing, or one may even observe decreasing apparent frequency. Frequency analysis is performed on the sequence of photos taken during the measurement. We define the limit of angular resolution where the dominant frequency reaches its upper limit (as seen later in Section V.B).

In case of HPO light-field displays, this measurement is performed in horizontal direction only. However, for 3D displays which have both a horizontal and vertical parallax, the measurement shall be repeated in a vertical direction to characterize the angular resolution in both directions. This is

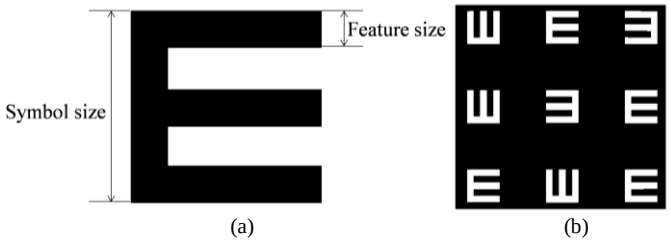

Fig. 6. Subjective spatial resolution test overview. (a) One tumbling "E" symbol. Feature size is 1/5 of the total symbol size. (b) A chart of 9 randomized E symbols arranged in a 3x3 matrix.

because horizontal and vertical angular resolution might be substantially different.

IV. Subjective Test of Perceived Spatial Resolution

For the case of angular resolution measurement, there is a direct way to verify the correctness of the results of our proposed methods, as discussed in Section III.C. However, there is no such direct method for the case of equivalent spatial resolution measurement. Therefore, we resort to designing and conducting a subjective test to corroborate the proposed objective measurements for that case.

A. Methodology of subjective test of perceived spatial resolution

In this test, the perceived spatial resolution of a light-field display is determined by showing visual features with various feature size to participants (see Fig. 6), and asking them to record what they can see on the screen. The visual feature chosen is the tumbling "E" symbol, which is often used by ophthalmologists to measure people's visual acuity [19], thus participants might already be familiar with them.

The methodology, as proposed, consists of two subsequent tests. The first test is done by using symbols printed on paper. It acts as pre-screening aimed at filtering participants with insufficient visual acuity. As such, it ensures that when in later tests people cannot recognize small symbols, this is caused by the peculiarities of the display, and not by the participant's limited visual acuity. In this first test, participants are asked to record the orientation of E's with randomized orientation, printed on paper, arranged in rows of 5, sized from 4 mm down to 0.85 mm, symbol size shrinking with 4/5 in 12 steps (halving every 3 steps), like in real tumbling E charts. From 80 cm viewing distance the 4 mm symbol size corresponds to 0.29 degree symbol size and 0.058 degree (~3.52 arcmins) feature size (also see Fig. 6 (a)). The smallest symbol size (0.8 mm) from the same distance corresponds to 3.69 minutes of arc, and a feature size of 0.73 minutes of arc. Only participants that pass the first test successfully (100% recognition of bigger symbols on paper) proceed to second test.

In the second test, people are presented with the 3D display at the same distance where the paper was shown. The display shows 9 randomized symbols, arranged in a 3 x 3 matrix (as shown in Fig. 6. (b)), and participants copy the orientation of the E's onto a 3x3 matrix on paper. 26 sets are presented in total and the first 4 are considered training sets, while the remaining 22 tests show 11 symbol sizes, both shown twice. Since we are not assessing the visual quality but the ability of the display to discriminate resolution variations, we use similar content for training and the actual experiment in order to allow people to familiarize with the test pattern and the task. The answers given for the training sets are not used during analysis. Symbol sizes are randomized to avoid habituation or anticipation that may affect results obtained by monotonically increasing or decreasing symbol sizes. The time elapsed between the presentation of a new set of symbols and reporting readiness (when all symbols have been recognized and recorded on paper) is measured and logged.

B. Analysis of subjective test of perceived spatial resolution

First the results of the paper-based visual acuity tests are calculated, based on which participants with insufficient visual acuity to perform the test are eliminated. After removing the training sets, the randomized pattern sizes are reordered based on the recorded log files, resulting in an ordered list of accuracy and completion time for all participants (except those who failed on the paper based visual acuity test) for 11 symbol sizes of decreasing feature size. The accuracy values for all participants are averaged and the standard deviations and the 95% confidence intervals over recognition data are calculated.

Our hypothesis is that the participants will correctly recognize the symbols up to a given symbol size that corresponds to perceived display resolution and start making significant mistakes (wrong guesses) once the symbols are below the resolution of the display. We aim to identify the subjectively perceived spatial resolution corresponding to the smallest feature size participants are still able to recognize properly. We also check whether the time spent to recognize the symbols increases significantly, which would indicate that the resolution limit has been reached (when participants have difficulties in recognizing symbol orientations).

Although common visual acuity tests determine the limit of visibility where recognition accuracy falls below 50%, as recommended by [19], recent results such as [20] suggest that there may be significant differences between the recognition accuracy of different symbols (optotypes) due to the fact that the unbalanced symbols can be recognized based on their luminance distribution, even if they are heavily blurred or distorted. This suggests that such a subjective test cannot practically determine an absolute limit of visibility. We aim, however, to relate the uncertainty of visibility with the objective measurements.

V. Results and Discussion

We demonstrate the applicability of the proposed measurement approaches on a light-field display. The display under test was a large-scale prototype light-field display with 180 cm screen diagonal. The display is controlled by a rendering cluster with high-end GPUs connected via HDMI connections. The setup for subjective experiments is described in Section V.C.

A. Spatial resolution measurement

During the measurement, 411 photos have been taken for both horizontal and vertical directions and analyzed as described in Section III.B. The analysis procedure has been implemented in

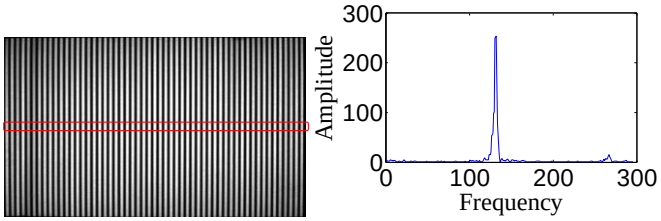

Fig. 7.(a) A photo of the screen showing a sinusoidal test pattern. The center row of the photo is used for frequency analysis. (b) Frequency spectrum of a single measurement showing the sinusoidal, with FFT bins on the horizontal axis.

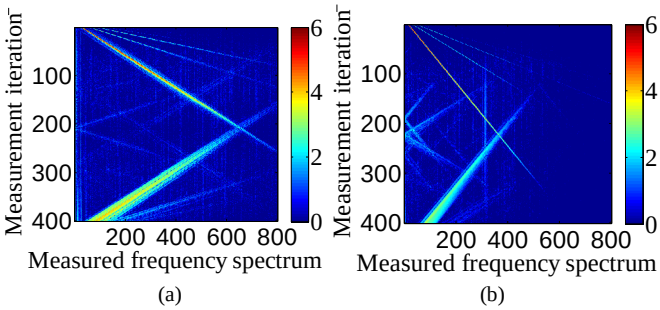

Fig. 8. Frequency spectrums of successive measurements stacked in a matrix. Measurement iteration count increases downwards, while the observed frequency increases rightwards. (a) Spectrums of horizontal resolution measurements. Major sources of distortion are visible as harmonics and constant low-frequency distortion. (b) Spectrums of vertical resolution measurements.

a Matlab script.

A photo of the light-field display showing a sinusoidal test pattern is shown in Fig. 7. (a). One line of samples is extracted from the center of the screen, on which 1D frequency analysis is performed. The frequency spectrum of a single measurement is shown in Fig. 7. (b), with FFT bins shown on the horizontal axis. How these relate to real resolution will be explained later in this section.

Using a series of photos and stacking the resulting frequency spectrums to form a 2D matrix, the frequency response of the display under test with increasing input frequencies is obtained, as shown in Fig. 8. Measurement iterations with increasing input frequency are shown on the vertical axis from top to bottom, while the resulting frequency spectrum is on the horizontal axis. The strong diagonal in the spectrum shows the input frequency being output by the display as the dominant frequency.

There are however other frequency components in the spectrum, the causes of which will be discussed. The decrease of the amplitude of the dominant signal is also visible on the diagonal. After finding the primary and secondary peak for all iterations, the ratio of the amplitude of the primary peak and the amplitude of the secondary peak can be plotted, which shows the level of distortion for each iteration. Such a plot is shown in Fig. 9, where distortion level is plotted in blue against the 20% threshold. From the plot one can see that the first iteration where distortion is above 20% is number 166.

The iteration number can be easily mapped to effective display resolution by plotting the frequency of the primary

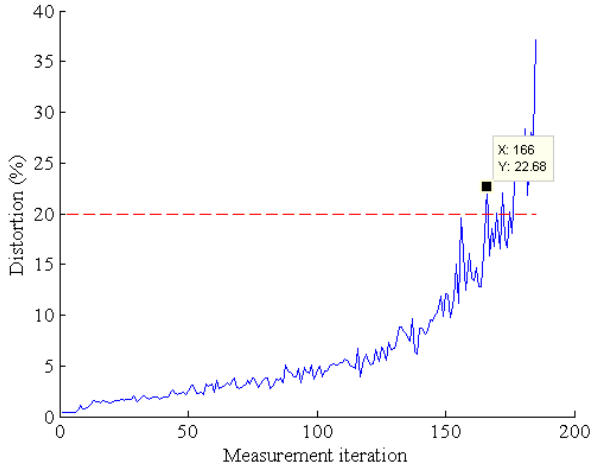

Fig. 9. Level of distortion in subsequent measurement iterations. 20% noise threshold is marked with red dashed line.

peak against the measurement iteration.

The resolution is the double of the measured frequency (529 in our case), as one period is considered to be created by the equivalent of two pixels per period in the classical discrete to analog signal conversion (one black and one white). Based on this correspondence between resolution and the frequency the horizontal resolution for the display under test is 2*(529-1) = 1056 pixels. One is subtracted from the frequency value, as the first bin in the spectrum corresponds to the DC component of the signal.

While determining the effective resolution is a useful result by itself, closely checking the stacked spectrums reveals some sources of distortion. Due to the slightly nonlinear intensity transfer function of the display, sinusoidals appear slightly rectangular, causing harmonics at odd multiples of the dominant frequency, appearing as weaker diagonals, as shown in Fig. 8. (a). Also, constant low frequency components on the left-hand side of the spectrum are visible in Fig. 8. (a). These are caused by the characteristic of the holographic screen, which results in slightly nonuniform brightness over the screen surface. This manifests itself in a fixed low frequency across all measurements.

Frequency aliasing can also be observed when exceeding the frequency throughput of the display with a large margin. Fig. 8. (b) shows the stacked spectrum of the vertical resolution of the measured display, which happens to be lower in the vertical direction. Starting around iteration 170, the mirrored image of the peak appears. Using the same calculation as with the horizontal resolution, the vertical resolution of the display is determined to be 636 pixels.

B. Angular resolution measurement

Results for the same light-field display as used for the spatial resolution measurement are presented below. During this measurement, 60 videos have been taken with increasing angular frequencies, and analyzed as described in Section III.D. Sample intensity profiles of two different frequencies are shown in Fig. 10. (a). Each curve corresponds to the intensity observed by the camera at the center of the captured

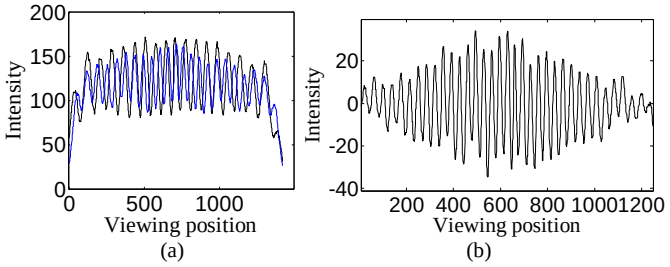

Fig. 10. (a) Sample intensity profiles for two different angular frequencies recorded on the same display. (b) Intensity profiles of forced black-white transitions on a light-field display.

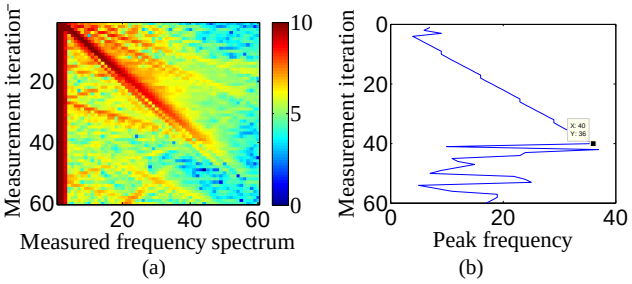

Fig. 11. (a) 1D frequency spectrums of angular resolution test patters stacked in a 2D array. (b) Frequency of the peak in subsequent measurement iterations.

image as the camera was moving sideways in front of the screen, showing a constant angular resolution test pattern.

By performing frequency analysis on each of the captured intensity profiles and stacking the spectrums below each other (as seen in Fig. 11. (a)), the increasing frequency of the test pattern can be clearly observed as a primary peak, with increasing frequency until approx. iteration 45. In subsequent iterations we can see the peak disappear and noise appear instead. Finding the peak in subsequent iterations (as shown in Fig. 11. (b)) gives the maximum number of periods one can observe over the field of view of the display. The peak in our case is at 36, which corresponds to 35 full periods (as the first bin in the spectrum corresponds to the DC component of the signal). The number of distinct directions is twice the number of full periods, in our case 70.

Dividing the total viewing angle of the display with this number, the angular resolution can be obtained. This display's total viewing angle is 65.4 degrees according to the measured intensity profile; therefore, the average angular resolution is 0.93 degrees.

Using the direct method for identifying the number of distinct directions that can be reproduced (as described in Section III.C), one can count 35 peaks on Fig. 10. (b), showing the intensity profile of the display under test. This alternative approach demonstrates that our method succeeded in finding the maximum number of directions emitted by the display.

C. Subjective test of perceived spatial resolution

Subjective tests have been performed on 53 participants, 43 male and 10 female. The age range of participants was between 22 and 52 years. 21 of them used glasses. All participants claimed to have good eye sight and this was

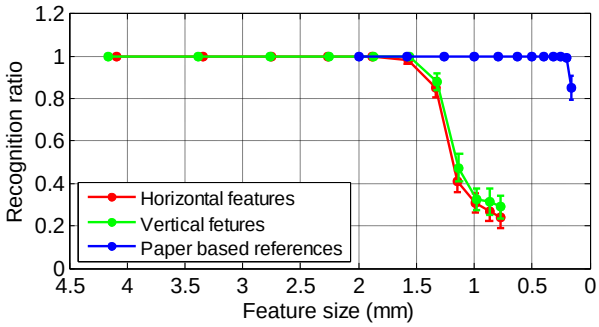

Fig.12. Recognition accuracy of tumbling E symbols on paper and display, for horizontal and vertical features, plotted against feature size, with 95% confidence intervals.

verified using the paper based charts as the first step of the tests. None of the participants were native English speakers (the study being performed in Finland), but represented several nationalities. We selected 50+ participants to participate in the subjective experiment in order to meet the requirements in the ITU Recommendation [21], that specifies that 'at least fifteen participants, non-experts, should be employed'. The distance between the display's screen and the participant's eye was 80 cm during the spatial resolution tests.

In our experiment, 3 out of 53 participants could not reliably record the orientation of the paper based patterns - those were removed from all analysis related to estimating the spatial resolution.

The weighted average of recognition accuracies and corresponding 95% confidence intervals have been calculated for all used symbol sizes for symbols with horizontal and vertical detail orientation (U/D and L/R). Based on symbol size, the feature sizes, and the corresponding resolution values for each symbol size have been calculated. Completion times have been averaged and 95% confidence intervals calculated. The averaged recognition accuracies are shown in Fig. 12. The figures clearly show several effects: the most obvious is that participants recognized the paper based reference almost perfectly (please note that the paper based symbols started smaller, though there is some overlap in symbol sizes). This means the limits visible in recognition accuracy in the case of the display are caused by the display's resolution limit, and not because of the participant's visual acuity limits.

The second noticeable result is that there is a statistically significant drop in recognition around feature size 1.4 mm: there, the confidence intervals do not overlap between measurement steps, and the p-values are very small ($p_{horizontal}$ = 3.91e-07, $p_{vertical}$ = 3.54e-07). This proves our hypothesis that there is a limit on the resolution the display is capable to visualize and it is close to symbol size where the recognition ratios have a major drop.

From charts in Fig. 13 and Fig. 14 it can be read that the measured resolution by the objective method (1056x636) corresponds to 93% and 92% recognition ratios in the horizontal and vertical direction, respectively. This is much higher than the 50% threshold commonly used in visual acuity tests, which can be attributed to the previously mentioned capability of humans recognizing symbols whose features are

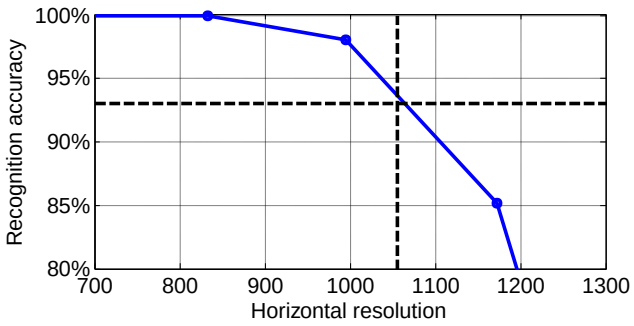

Fig.13. Zoomed in version of recognition accuracy versus resolution plot for horizontal resolution

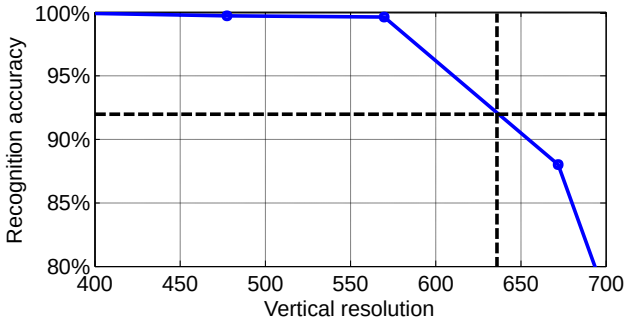

Fig.14. Zoomed in version of recognition accuracy versus resolution plot for vertical resolution

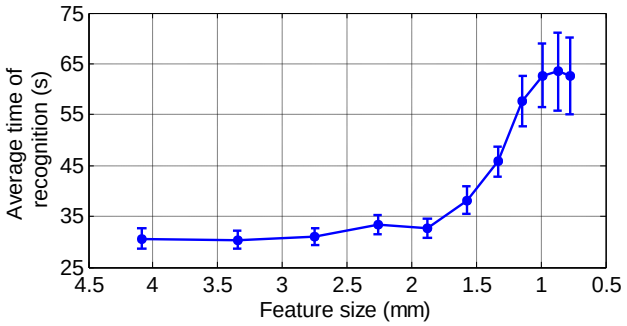

Fig.15. Average recognition time for a group of symbols with given feature size

not entirely visible [20][22][23]. Still, the thresholds being so close in the horizontal and vertical directions indicate that the measured resolution values and subjective perception of the visible features are proportional. From a practical perspective, this means that if a content producer provides content complying with the measured spatial resolution, this will ensure good suppression of visually annoying 3D artifacts for the greatest majority of viewers.

Note that the way of carrying out the subjective experiments imposed the use of certain finite set of symbol sizes. Therefore, we used linear interpolation between measured values to estimate the expected recognition accuracy for intermediate resolutions.

A summary of times participants needed to perform each iteration of the test are shown in Fig. 15. It is clearly visible that the average time to recognize and record a group of symbols stays almost constant until feature size ~1.4 mm. Symbols smaller than this limit seem to be increasingly difficult to recognize, indicated by the increased average recognition time as well as the larger confidence intervals. Incidentally, the resolution limit obtained by the objective method is reached at this feature size respectively. This shows that a steep increase in recognition time also indicates that the limit of visibility has been reached.

VI. Conclusions

This paper addressed the proper characterization of light-field 3D displays. Two important limiting factors, namely spatial and angular resolution have been discussed, and camera-based objective measurement methodologies have been proposed. A subjective test for corroborating the results of the spatial resolution measurement has also been proposed. These measurement methods and subjective tests have been performed on a light-field display. We have identified limiting factors in light-field displays and how these manifest themselves in the measurements, and how human participants react when these limits are reached. Using the proposed measurement methods, light-field displays can be objectively quantified.

Further work will address any of the advancements over the methods presented here, such as: measuring the perceived resolution on depth planes different from the screen plane; the detection of potential non-uniformities in spatial and angular resolution; or the reduction of measurement time by using smaller number of photos to find the limits.

References

[1] M. S. Banks, D. M. Hoffman, J. Kim, G. Wetzstein, “3D Displays,” *Annual Review of Vision Science*, vol. 2, pp. 397-435, Oct. 2016.

[2] C. van Berkel, D. W. Parker, A. R. Franklin, “Multiview 3D-LCD,” *Proc. SPIE 2653, Stereoscopic Displays and Virtual Reality Systems III*, Apr. 1996

[3] T. Balogh, “The HoloVizio system,” in *Proc. SPIE 6055, Stereoscopic Displays and Applications XIII*, 60550U, Jan. 2006.

[4] G. Wetzstein, D. Lanman, M. Hirsch, R. Raskar, “Tensor Displays: Compressive Light Field Synthesis using Multilayer Displays with Directional Backlighting,” *ACM Trans. Graphics, Proc. SIGGRAPH 2012*, vol. 31, no. 4, Jul. 2012.

[5] J.-H. Lee, J. Park, D. Nam, S.-Y. Choi, D.-S. Park, C.-Y. Kim, “Optimal Projector Configuration Design for 300-Mpixel Light-Field 3D Display,” *Optics Express*, vol. 21, no. 22, pp. 26820-26835, 2013.

[6] M. Kawakita, S. Iwasawa, R. Lopez-Gulliver, M. Makino, M. Chikama, M. P. Tehrani, “Glasses-free 200-view 3D Video System for Highly Realistic Communication,” *Proc. Digital Holography and Three-Dimensional Imaging 2013*, Apr. 2013, pp. DM2A.1.

[7] A. Stern, Y. Yitzhaky, B. Javidi, "Perceivable Light Fields: Matching the Requirements Between the Human Visual System and Autostereoscopic 3-D Displays," *Proc. of the IEEE*, vol. 102, no. 10, pp. 1571-1587, Oct. 2014.

[8] G. Wu, B. Masia, A. Jarabo, Y. Zhang, L. Wong, Q. Dai, T. Chai, Y. Liu, “Light field image processing: An Overview,” *IEEE Journal of Selected Topics in Signal Processing*, 2017

[9] R. Bregović, P. T. Kovács, A. Gotchev, “Optimization of light field display-camera configuration based on display properties in spectral domain,” *Optics Express*, vol. 24, no. 3, pp. 3067-3088, Feb. 2016.

[10] M. Zwicker, W. Matusik, F. Durand, H. Pfister, C. Forlines, “Antialiasing for automultiscopic 3D displays,” *ACM Trans. Graphics, Proc. SIGGRAPH 2006*, Aug. 2006.

[11] A. Boev, R. Bregovic, A. Gotchev, “Measuring and modeling per-element angular visibility in multi-view displays,” *Journal of the Society for Information Display*, vol. 18, no. 9, pp. 686–697, Sep. 2010.

[12] P. Boher, T. Leroux, T. Bignon, V. Colomb-Patton, “A new way to characterize autostereoscopic 3D displays using Fourier optics

instrument," *Proc. SPIE 7237, Stereoscopic Displays and Applications XX*, 72370Z, Feb. 2009
[13] The International Display Measurement Standard v1.03, Society for Information Display, 2012.
[14] P. T. Kovács, A. Boev, R. Bregović, A. Gotchev, "Quality measurements of 3D light-field displays," *Proc. 8th Int. Workshop on Video Processing and Quality Metrics for Consumer Electronics 2014*, Jan. 2014.
[15] A. Boev, R. Bregović, A. Gotchev, "Visual-quality evaluation methodology for multiview displays," *Displays*, vol. 33, no. 2, pp. 103-112, Apr. 2012.
[16] L. Wang, K. Teunissen, T. Yan, C. Li, Z. Panpan, Z. Tingting, I. Heynderickx, "Crosstalk Evaluation in Stereoscopic Displays," *Display Technology*, vol. 7, no. 4, pp. 208-214, Mar. 2011.
[17] P. J. H. Seuntiëns, L. M. J. Meesters, W. A. IJsselsteijn, "Perceptual attributes of crosstalk in 3D images," *Displays*, vol. 26, no. 4-5, pp. 177-183, Oct. 2005.
[18] F. Kooi, A. Toet. "Visual comfort of binocular and 3D displays," *Displays*, vol. 25, no. 2-3, pp. 99–108. Aug. 2004.
[19] International Society for Low vision Research and Rehabilitation, "Guide for the Evaluation of Visual Impairment," *Proc. International Low Vision Conference (VISION-99)*, Jul. 1999.
[20] S. P. Heinrich, M. Back, "Resolution acuity versus recognition acuity with Landolt-style optotypes," *Graefes Arch Clin Exp Ophthalmol*, vol. 251, no. 9. pp. 2235–2241, Sep. 2013.
[21] Methodology for the subjective assessment of the quality of television pictures, ITU-R BT.500-13, Jan. 2012.
[22] J. S. Pointer, "Recognition versus Resolution: a Comparison of Visual Acuity Results Using Two Alternative Test Chart Optotype," *J Optom* 2008, vol 1, pp. 65-70. 2008
[23] L. N. Reich, M Ekabutr, "The Effects of Optical Defocus on the Legibility of the Tumbling-E and Landolt-C," *Optometry and Vision Science*, vol. 79, no. 6, pp. 389–393

Péter Tamás Kovács (Student member, IEEE) received the M.Sc. degree in computer science from the Budapest University of Technology, Budapest, Hungary in 2004. He is currently pursuing the Ph.D. degree in signal processing at Tampere University of technology, Tampere, Finland.

From 2004 to 2006, he was a Software Engineer with Archi-Data. Since 2006, he has been Software Engineer, Lead Software Engineer, then CTO of Holografika. He has been a visiting researcher at Tampere University of Technology from 2013 to 2014. He is the author or co-author of four book chapters, four journal papers and more than 30 conference papers. His research interests include 3D displays, more specifically light-field displays, and the capture / compression / rendering of light fields.

He has served as PC member for numerous IEEE conferences, Local Organizing Chair of 3DTV-Con 2014, and is a contributing member of the International 3D Society and the International Committee for Display Metrology (ICDM), where he contributed to the first IDMS standard. He was the Head of Delegation to MPEG for Hungary.

Robert Bregović (Member, IEEE) received the Dipl. Ing. and MSc degrees in electrical engineering from University of Zagreb, Zagreb, Croatia, in 1994 and 1998, respectively, and the Dr. Sc. (Tech.) degree (with honors) in information technology from Tampere University of Technology, Tampere, Finland, in 2003.

From 1994 to 1998, he was with the Department of Electronic Systems and Information Processing of the Faculty of Electrical Engineering and Computing, University of Zagreb. Since 1998, he is with the Laboratory of Signal Processing, Tampere University of Technology. His research interests include the design and implementation of digital filters and filterbanks, multirate signal processing, and topics related to acquisition, processing, modeling, and visualization of 3D content.

Atanas Boev is a researcher with expertise in light field displays and human stereopsis. He got the best demo award at Tampere Innovation Days 2010, best student paper award in Electronic Imaging 2011, and Nokia Scolarship award in 2010. He defended his PhD in Tampere University of Technology, Finland in 2012. In 2013 he was visiting researcher at Holografika KFT, Hungary, doing development and implementation of light field rendering algorithms. In 2014 he was post-doctoral researcher in Tampere University of Technology working on modern signal processing methods for lightfield displays. Currently, he is a research engineer in the Huawei European Research Centre, working on light field display technology.

Attila Barsi received the M.Sc. degree in computer science from the Budapest University of Technology, Budapest, Hungary in 2004.

From 2005 to 2006, he was a Software Engineer with DSS Hungary. Since 2006, he has been Software Engineer, then Lead Software Engineer of Holografika. He is the author or co-author of several conference and journal papers. His research interests include light fields, real-time rendering, ray tracing, global illumination and GPU computing.

Atanas Gotchev (Member, IEEE) received the M.Sc. degrees in radio and television engineering (1990) and applied mathematics (1992) and the Ph.D. degree in telecommunications (1996) from the Technical University of Sofia, and the D.Sc.(Tech.) degree in information technologies from the Tampere University of Technology (2003).

He is a Professor at the Laboratory of Signal Processing and Director of the Centre for Immersive Visual Technologies at Tampere University of Technology. His research interests have been in sampling and interpolation theory, and spline and spectral methods with applications to multidimensional signal analysis. His recent work concentrates on algorithms for multisensor 3-D scene capture, transform-domain light-field reconstruction, and Fourier analysis of 3-D displays.